

EFFECT OF SHAPE AND WETTABILITY OF PACKING MATERIALS ON THE EFFICIENCY OF PACKED COLUMN

Myung-Wan Han, Dae-Ki Choi and Won Kook Lee*

Dept. of Chem. Eng. KAIST

(Received 15 June 1984 • accepted 21 August 1984)

Abstract — Effective interfacial area and mass transfer coefficient were determined by the use of Danckwerts' plot method for chemical absorption system accompanied by first order reaction to elucidate the effect of shape and wettability of packing materials on these parameters.

The liquid phase used in this experiment was K_2CO_3 - $KHCO_3$ buffer solution, and $NaOCl$ was used to catalyze the first order reaction in the liquid phase. Raschig ring, square, sphere in shapes, and these were made of ceramic, polypropylene, glass, stainless steel, were used as packing materials.

The following correlations were obtained to predict the effective interfacial area and mass transfer coefficient.

$$a/a_t = 0.614 Re^{0.161} (\sigma_c/\sigma)^{0.119} (a_t d_n (1 - \epsilon)^{\frac{1}{3}})^{-1.01}$$

$$K_L = 0.0154 Re^{0.24} (\sigma_c/\sigma)^{0.48} (a_t d_n)^{0.19}$$

INTRODUCTION

Packed columns are widely used for gas absorption, liquid extraction and distillation etc. in the chemical plants. In a packed-column absorber, the liquid flows down over the packing surface as film and the gas passes through the space between the packings while mass transfer occurs at the interphase.

Packing material is the most important part of the operation, and its main role is to increase the contacting area where the mass transfer occurs.

The efficiency of packed column may be well represented by two parameters, i.e., mass transfer coefficient and effective interfacial area. The shape and wettability of packing materials have a close relation with these two parameters.

The effect of the shape of packing materials on them has been investigated by many researchers. Shulman [11] observed that the wetted area increases but the effective interfacial area decreases with the size of packings. Sahay and Sharma [10] found that polypropylene Pall ring showed the lower values of the effective interfacial area than polypropylene Intalox saddles and P.V.C. Raschig rings. They suggested that it may be so because the construction of the Pall ring does not offer continuous surface for the liquid stream to be spread on its surface. Puranik and Vogelpohl [9] assumed that the shape of packing can be characterized by dry surface

area per unit volume only. Lee [5] insisted that void fraction also should be considered.

The investigation about the effect of material of packing on column efficiency began with the practical usage of packings made of plastic. Coughlin [2] reported that ceramic packings have an K_L a 25% greater than plastic packings. Onda et al. [7] introduced the concept of critical surface tension to characterize the wetting behavior. Puranik and Vogelpohl [9] used the critical surface tension to the effect of the nature of packing on its effective area.

Purpose of this work is to found the better prediction equations for the effective interfacial area and the mass transfer coefficient from the operating parameters and physical properties of the system.

THEORETICAL BACKGROUND

In absorption system accompanied with a first order reaction, its governing equation may be expressed as the following.

$$\frac{\partial A}{\partial \theta} = D \frac{\partial^2 A}{\partial x^2} - K_L A \quad (1)$$

Its boundary conditions are

$$\begin{aligned} A &= 0, & X > 0, & \theta = 0 \\ A &= A^*, & X = 0, & \theta > 0 \\ A &= 0, & X = \infty, & \theta > 0 \end{aligned} \quad (2)$$

* To whom correspondence should be addressed.

Through the Laplace transform, its solution can be obtained.

$$\bar{A} = A^* \exp -x/D \sqrt{DK_1 + K_L^2} \quad (3)$$

Danckwerts(3) proposed the surface renewal model assuming that the liquid element at the surface is displaced with the fresh liquid element in bulk and has an age distribution from zero to infinite.

In Danckwerts' model, the average absorption rate per unit area is

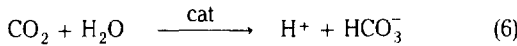
$$\begin{aligned} \bar{R} &= s \int_0^{\infty} R e^{-s\theta} d\theta \\ &= -D \left(\frac{d\bar{A}}{dx} \right)_{x=0} \\ &= A^* \sqrt{K_L^2 + DK_1} \end{aligned} \quad (4)$$

This equation may be rearranged into a following form.

$$\left(\frac{\bar{R}}{A^* \sqrt{D}} \right)^2 = a^2 K_1 + \frac{(K_L a)^2}{D} \quad (5)$$

The reaction rate constant K_1 can be changed using a catalyst. Consequently, effective interfacial area and mass transfer coefficient can be obtained from its slope and intercept after plotting the $(\bar{R}/A^* \sqrt{D})^2$ against K_1 . (Danckwerts' plot)

In this system, the overall reaction rate of CO_2 is controlled by the catalytic reaction.



Rate equation has the following form when NaOCl is used as the catalyst.

$$r = K_1 [\text{CO}_2] \quad (7)$$

$$\text{where } K_1 = K_{\text{H}_2\text{O}} + K_{\text{OCl}^-} [\text{OCl}^-]$$

Phorecki(8) found that the dependence of K_{OCl^-} on the composition of solution may be expressed by following equation.

Table 1. Characteristics of packing materials.

Packing	Shape	Raschig Ring			Square			Sphere	
	Material	p. p	Ceramic	Glass	p. p	Ceramic	Stainless steel	p. p	Ceramic
height (cm)		1. 25	1. 25	1. 25	1. 239	1. 240	1. 25	-	-
diameter or length		1. 25	1. 25	1. 25	1. 317	1. 317	1. 25	1. 258	1. 258
thickness (cm)		0. 18	0. 25	0. 1	0. 158	0. 235	0. 1	-	-
dry surface area/packing (cm^2)		9. 614	9. 853	9. 816	12. 32	12. 70	12. 42	4. 971	5. 366
packing density		0. 389	0. 355	0. 404	0. 300	0. 291	0. 289	0. 574	0. 513
volumetric surface area (cm^2/cm^3)		3. 740	3. 498	3. 956	3. 696	3. 696	3. 589	2. 853	2. 753
void fraction		0. 706	0. 651	0. 854	0. 74	0. 633	0. 834	0. 402	0. 400

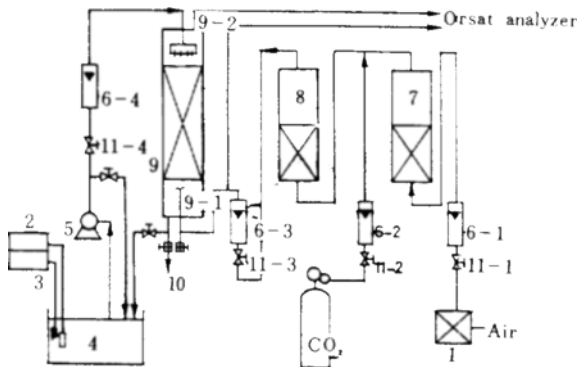


Fig. 1. Schematic diagram of experimental apparatus.

1. air regulator	2. cooler
3. constant temp. circulator	
4. feed tank	5. feed pump
6. rotameters	7. CO_2 absorber
8. humidifier	9. packed column
10. output liquid sampler	11. needle valves

$$K_{\text{OCl}^-} = 1518 + 1318 [\text{CO}_3^{2-}] / \text{HCO}_3^- \quad (8)$$

EXPERIMENTAL

Schematic diagram of experimental apparatus is illustrated in Fig. 1. Compressed air was used for the gas phase and carbon dioxide contained in it was removed by passing through the CO_2 removal column(7) and mixed with pure CO_2 gas from CO_2 cylinder.

The mixed gas was saturated in the humidifier (8) and, before going into the bottom of the main packed column, sampled and checked with Orsat analyzer. The main packed column was made of acryl column of 10

Table 2. Operating condition.

Liquid viscosity	1. 25 - 1. 313 c. p
Liquid density	1. 17 - 1. 19 g/cm ³
Liquid temperature	21 ± 0. 5°C
Packing height	54 cm
Gas velocity	160 cm ³ /sec
Superficial liquid velocity	0 - 1. 2 cm/sec
(K ₂ CO ₃)	0. 6 - 0. 45 g mol/l
(KHCO ₃)	0. 25 - 0. 5 g mol/l
(KCl)	1. 94 ± 0. 03 g mol/l
(NaOCl)	0 - 0. 2 g mol/l
pH of the liquid	10. 2 - 10. 1
CO ₂ partial pressure	
of inlet gas	0. 1 atm
Total pressure	1 atm

cm inside diameter. In each operation, the flow rate of gas was controlled by using needle valves (11) and rotameters (6).

On the other hand, the liquid phase was potassium carbonate-bicarbonate buffer solution, and was kept at 21 ± 0.5°C with the constant temperature circulator (3) and immersion cooler (2) in the feed tank (4). The liquid was drawn up with feed pump (5) to the top of the packing and evenly distributed through the distributor (9-2) and run down over the packing. Therefore it came into contact with the gas rising from the bottom of the column.

Packing materials used in this experiment and its characteristics are shown in Table 1. Operating conditions of this system are listed in Table 2. Potassium chloride was used to keep the physical properties of the buffer solution constant. Sodium hypochlorite was added as a catalyst to change the reaction rate constant. The reaction rate constant was determined using the equation reported by Phorecki [8].

This experiment was performed with changing the superficial liquid velocity and the packing material.

RESULTS AND DISCUSSION

Effective interfacial area and liquid side mass transfer coefficient were determined by Danckwerts' plot method. Fig. 2 is an example of Danckwerts' plot.

(1) The effect of the shape of packing material on effective area.

Nominal size(d_n), dry surface area per unit volume(a) and void fraction(ϵ) were first considered to characterize the effect of shape of packing on effective

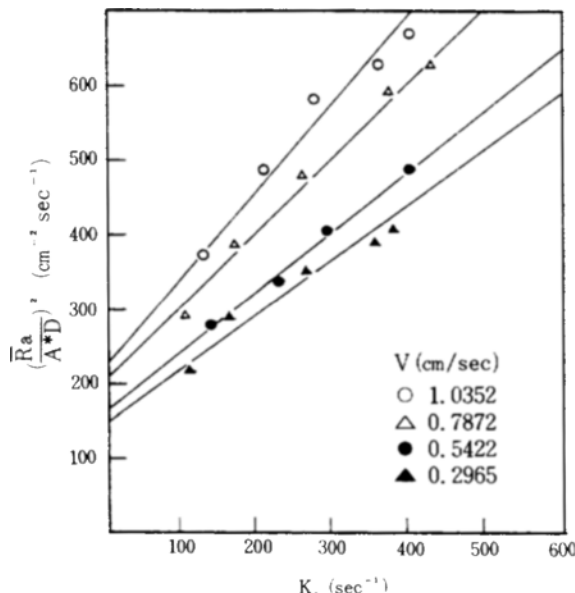


Fig. 2. Danckwerts' plot for $\frac{1}{2}$ " P. P. Raschig Ring at various superficial liquid velocities.

interfacial area. The relation of these variables with the effective interfacial area was checked with the regression analysis of the experimental data, and packing factor, $a/d_n(1-\epsilon)^{1/3}$, could be formed by considering the exponent of these variables in the correlation. In Fig. 3, $\ln(a/a_t)$ is plotted against the packing factor, and its slope is -1 approximately. In this regard, it shows that a/a_t decreases with dry surface area per unit volume and increases with void fraction. However, when the effective interfacial area is only taken into account, it appears that the effective area is mainly affected by void fraction.

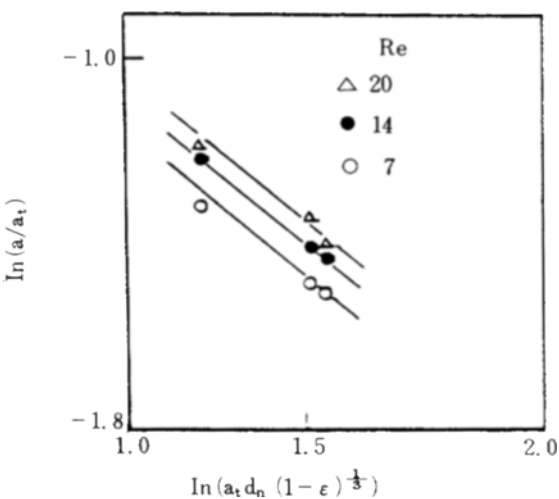


Fig. 3. Dependence a/a_t on $a_t d_n (1 - \epsilon)^{1/3}$

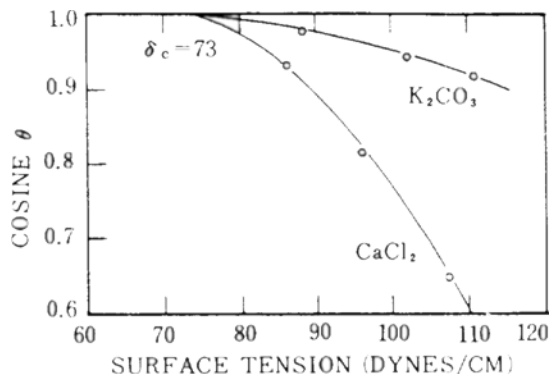


Fig. 4. Surface tensions of aqueous solutions of potassium carbonate and calcium chloride vs. cosine of the contact angle (6).

The fact seems to support the suggestion of Lee [5]. He insisted that when void fraction is small, the space between the packing can be easily filled up by the liquid and in its consequence, the contacting area decreases.

(2) Effect of the wettability of packing materials on effective interfacial area.

Contact angle is well explained the wetting interaction between solid and liquid. This angle may be represented as a function of each different interfacial tensions.

$$\cos \theta = \frac{\nu_{LV} - \nu_{SL}}{\nu_{LV}}$$

where, ν_{SL} : solid-liquid interfacial tension
 ν_{LV} : liquid-vapor interfacial tension

Onda et al. [7] introduced the concept of critical surface

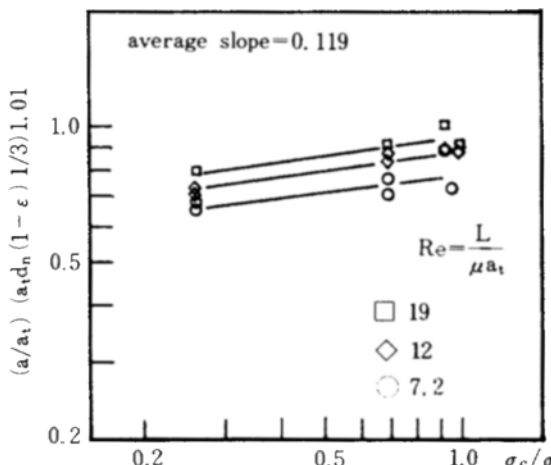


Fig. 5. Dependence of $(a/a_t) (a_t d_n (1 - \epsilon)^{-1/3})^{1.01}$ on (σ_c / σ) .

Table 3. Values of critical surface tension of various packing materials [Onda et al.(7)].

Material	$\sigma_c (10^{-2} \text{ kg S}^{-1})$
Glass	7.3
Ceramic	6.1
PVC	4.0
Carbon	6.0 - 6.5
Steel	7.1
Paraffin	2.0

tension to characterize the effect of the contact angle on its effective interfacial area. Here, critical surface tension is the maximum surface tension which permits the spread of the liquid on the packing. Fig. 4 shows the relation of the contact angle with surface tension of the liquids when the packing material is glass. From this diagram, it can be assumed that $\cos \theta$ is a function of the critical surface tension and surface tension of the liquid. The value of $\cos \theta$ approaches to 1, ie, wettability increases with the critical surface tension increasing and surface tension of the liquids decreasing as shown in this figure. It follows that the wetting behavior can be allowed to be explained by the ratio of the critical surface tension and surface tension of the liquid ie, σ_c / σ . The values of critical surface tension of various packing materials are listed in Table 3.

Fig. 5 shows the dependence of effective interfacial area on critical surface tension of the packing, where $[a_t d_n (1 - \epsilon)^{1/3}]^{1.01}$ takes into account the shape of packing. It shows that the wetting behavior between solid and liquid can be well explained with σ_c / σ .

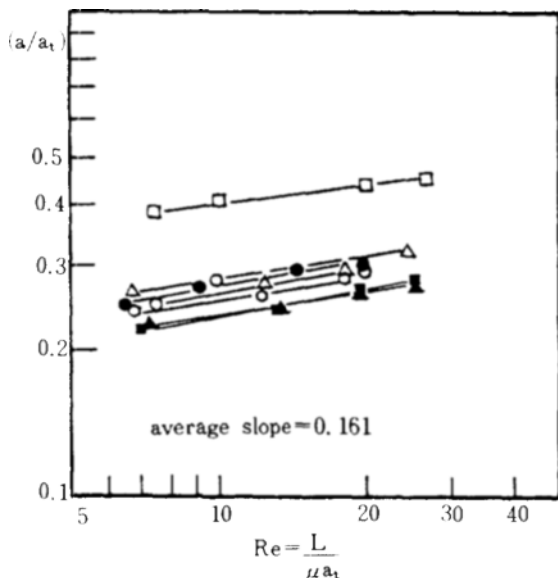
(3) The effective interfacial area (a/a_t)

a/a_t was correlated with three dimensionless groups. The dimensionless groups were discussed in the previous section.

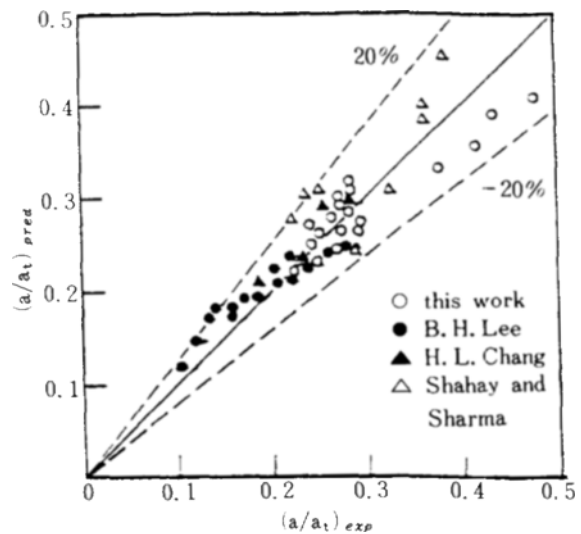
$$a/a_t = 0.614 \text{ Re}^{0.161} (\sigma_c / \sigma)^{0.119} (a_t d_n (1 - \epsilon)^{-1/3})^{-1.01}$$

The first term of the right hand side represents the operating effect the second and third terms characterize the wetting behavior and the shape effect of packing, respectively. In Fig. 6, a/a_t is plotted against Re . Its slope is in good agreement with the exponent of Re in the correlation. Predicted values of a/a_t by the correlation were compared in Fig. 7 with the experimental data. It is in good agreement within +20%, -15%. For checking the validity of the correlation, the values predicted are plotted against the experimental value of this work, B.H. Lee [5], H.L. Chang [1] and Sahay and Sharma [10] in Fig. 8. This also shows the good agreement with them.

(4) The mass transfer coefficient (k_L)

Fig. 6. Dependence of a/a_t on Re .

○ Ceramic Sphere	○ Ceramic R. R.
□ S. S. Square	▲ P. P. square
■ P. P. Raschig Ring	△ Glass R. R.
● P. P. Sphere	

Fig. 8. Comparison of $(a/a_t)_\text{pred}$ with the experimental data from this work and literature.

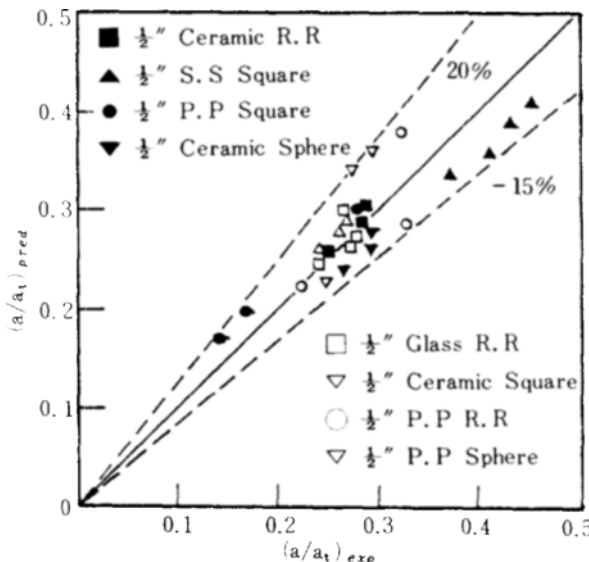
was performed.

$$k_L = 0.0154 (Re_f)^{0.24} (\sigma_c/\sigma)^{0.48} (a_t d_n)^{0.19}$$

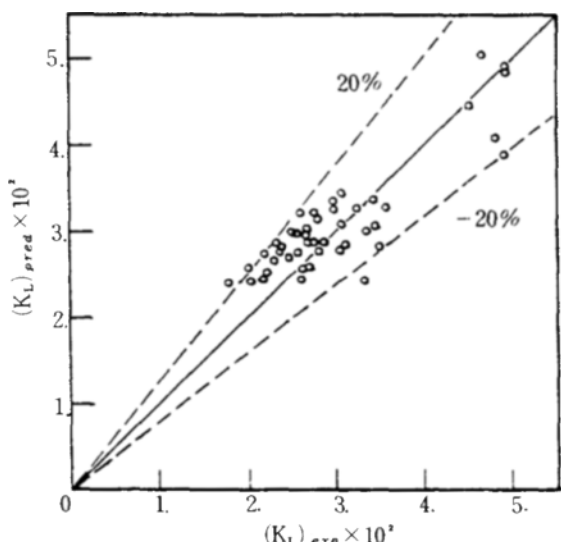
The mass transfer coefficient predicted from the correlation and its experimental data are compared in Fig. 9.

(5) The volumetric mass transfer coefficient ($k_L a$)

Values of $k_L a$ for the various packings and solutions are plotted in Fig. 10. The values in chemical absorption are larger than those in physical absorption. It seems due to the fact that the absorption process can not be continued at the semi-stagnant pools and very thin liquid film in the case of physical absorption. Because

Fig. 7. Comparison of $(a/a_t)_\text{pred}$ with the experimental data.

In the same way, the liquid side mass transfer coefficient was correlated with three dimensionless groups. They are film Reynolds number, σ_c/σ , $a_t d_n$. Here, void fraction term was neglected because its effect on mass transfer coefficient was small when regression analysis

Fig. 9. Comparison of $(K_L)_\text{pred}$ with $(K_L)_\text{exp}$.

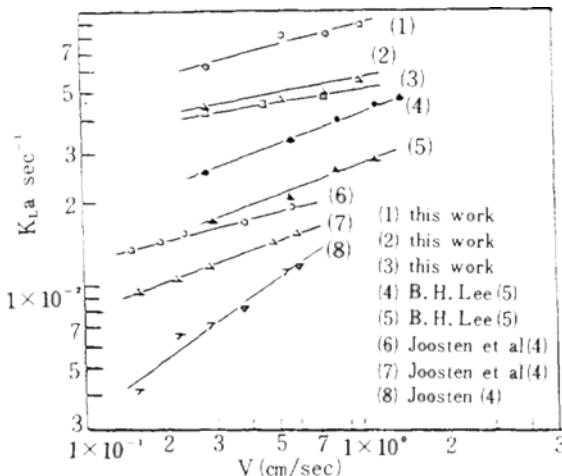


Fig. 10. Comparison of volumetric mass transfer coefficient in this work with that from others' data.

1. carbonate buffer (1/2" glass R. R.) $\mu = 1.28$ c. p
2. carbonate buffer (1/2" P. P. R. R.) $\mu = 1.28$ c. p
3. carbonate buffer (1/2" ceramic R. R.) $\mu = 1.28$ c. p
4. carbonate buffer (3/8" P. P. half R. R.) $\mu = 1.29$ c. p
5. carbonate buffer (3/8" P. P. half square) $\mu = 1.29$ c. p
6. carbonate buffer (1/2" ceramic R. R.) $\mu = 1.49$ c. p
7. carbonate buffer (1/2" ceramic intalox saddle) $\mu = 1.49$ c. p
8. inert solution (1/2" ceramic R. R.) $\mu = 1.49$ c. p

these regions are easily saturated and therefore act no role in mass transfer. The solid phase wettability of packing materials is found to have a considerable influence on $k_L a$. Fig. 10 shows $k_L a$ increases with the critical surface tension. It follows that liquid flow rate, solid phase wettability of packing and participation of chemical reaction may be thought to be influential factors on determining the volumetric mass transfer coefficient.

CONCLUSION

The efficiency of packed column may be well represented by two parameters, ie., the mass transfer coefficient and the effective interfacial area. Dependence of these two parameters on the shape and wettability of packing materials was considered. These two parameters were correlated with the dimensionless groups as follows:

$$a/a_t = 0.614 Re^{0.161} (\sigma_c/\sigma)^{0.219} (a_t d_n (1-\epsilon)^{1/3})^{-1.01}$$

$$k_L = 0.0154 (Re)^{0.24} (\sigma_c/\sigma)^{0.48} (a_t d_n)^{0.19}$$

It was found that the void fraction has a considerable in-

fluence on effective interfacial area, but a little effect on mass transfer coefficient.

The wetting behavior was well explained by critical surface tension.

NOMENCLATURE

A : concentration of dissolved gas (g mol/cm³)
Ā : Laplace transform of A (g mol/cm³)
a : effective interfacial area per unit volume (cm⁻¹)
a_t : dry surface area of packing per unit volume (cm⁻¹)
A* : concentration of dissolved gas at interphase (g mol/cm³)
d_n : nominal size of packing (cm)
D : diffusivity of solute
K₁ : first order reaction rate constant (sec⁻¹)
K_L : liquid side mass transfer coefficient (cm/sec)
L : superficial mass velocity of liquid (g/cm² sec)
r : rate of reaction of soluble gas per unit volume (g mol/cm³ sec)
R : rate of absorption per unit area of surface (g mol/cm² sec)
s : fractional rate of surface renewal (sec⁻¹)
x : distance beneath the liquid surface (cm)

Greek Letters

θ : contact time (sec)
μ : liquid viscosity (g/cm · sec)
ε : void fraction
σ : surface tension of liquid
σ_c : critical surface tension of the packing material (dyne/cm)

Dimensionless Group

Re : Reynolds number ($L/\mu a$)
Re_f : film Reynolds number ($L/\mu a$)

Abbreviation

P.P. : Polypropylene
R.R. : Raschig Ring
S.S. : Stainless Steel

REFERENCES

1. Chang, H.L.: M.S. Thesis, KAIST (1977).
2. Coughlin, R.W.: *AIChE J.*, **5**, 654 (1969).
3. Danckwerts, P.V.: "Gas-Liquid Reaction", McGraw-Hill, N.Y. 1970.
4. Joosten, G.E.H., and Danckwerts, P.V.: *Chem. Eng. Sci.*, **28**, 453 (1973).
5. Lee, B.H.: M.S. Thesis, KAIST (1979).
6. Olsen, D.A. and Osteraas, A.J.: *J. Phys. Chem.* **68**, 2730 (1964).

7. Onda, K., H. Takeuchi and Koyama, Y.: *Kagaku-Kogaku*, **31**, 126 (1967).
8. Pohoreski, R.: *Chem. Eng. Sci.*, **31**, 637 (1976).
9. Puranik, S.S., and Vogelpohl, A.: *Chem. Eng. Sci.*, **29**, 501 (1974).
10. Sahay, B.N., and Sharma, M.M.: *Chem. Eng. Sci.*, **28**, 41 (1973).
11. Shulman, H.L., Vllicht, C.F. and Wells, N.: *AIChE J.*, **1**, 247 (1955).